Synthesis and Characterization of Tricalcium Phosphate as Food Additives Derived from Gastropod (*Murex* sp.) Shell Waste

Malik Ali-Muhammad[1], Tatchai Pussayanavin[2] and Chalor Jarusutthirak[1*]

ABSTRACT

The gastropod (*Murex* sp.) shell is primarily composed of naturally formed calcium carbonate ($CaCO_3$). This research aimed to utilize $CaCO_3$ and calcium oxide (CaO) derived from gastropod shell waste for the synthesis of tricalcium phosphate (TCP) as food additives. The study focused on selecting appropriate starting materials and sustainable production processes. Initially, the shell waste was washed and dried before being heated at different temperatures: 300 °C to obtain $CaCO_3$ and 900 °C to obtain CaO. Subsequently, dicalcium phosphate (DCP) was synthesized by mixing $CaCO_3$ with phosphoric acid (H_3PO_4) until reaching a pH of 5. Finally, TCP was synthesized using a solid-state reaction method by mixing $CaCO_3$ or CaO with DCP at a ratio of 1:2, then calcining the mixture at 900 °C. All obtained composites, including $CaCO_3$, CaO, DCP, and TCP (synthesized from two alternative starting materials), were characterized using a total organic carbon (TOC) analyzer, Fourier transform infrared spectrometer (FT-IR), X-ray fluorescence spectrometer (XRF), X-ray diffractometer (XRD), and simultaneous thermogravimetric analyzer (STA). The results indicated the presence of the desired substances. Life cycle assessment (LCA) was used as a tool to compare the environmental impacts of TCP synthesis using two alternative materials derived from gastropod shell waste. The results proved that TCP synthesized from $CaCO_3$ exhibited more sustainable production processes and lower environmental impacts than TCP synthesized from CaO.

Keywords: Biowaste, Calcium carbonate, Dicalcium phosphate, Life cycle assessment, Tricalcium phosphate

INTRODUCTION

A million tonnes of calcium-rich waste from fisheries and seafood industries are generated globally every year, resulting in huge amounts of bio-waste from marine carcasses, especially seashell waste. More than 6,000 tonnes of marine shellfish are captured each year by artisanal fisheries (Department of Fisheries, 2022). Among these, large quantities of gastropod (*Murex* sp.) shells are discarded annually because they are not as popular as bivalve shells, leading to negative environmental impacts, including coastal pollution, landscape damage, unpleasant odors, and health problems (el Biriane and Barbachi, 2021). Gastropod shells are mainly composed of $CaCO_3$ in the forms of aragonite and calcite, with some trace metals and an organic matrix enhancing shell strength (Azarian and Sutapun, 2022; Iglikowska *et al*., 2023). Some literatures report the utilization of $CaCO_3$ derived from shells for various purposes (Ramakrishna *et al*., 2018; Yinka *et al*., 2020). For instance, $CaCO_3$ from abalone shells mixed with coffee waste has been utilized as fertilizer, while the conversion of $CaCO_3$ to ß-tricalcium phosphate (ß-$Ca_3(PO_4)_2$, ß-TCP) has been applied as a bone transplantation

[1]Department of Environmental Technology and Management, Faculty of Environment, Kasetsart University, Bangkok, Thailand
[2]Department of Environmental Science, Faculty of Science, Ramkhamhaeng University, Bangkok, Thailand
[*]Corresponding author. E-mail address: ecclj@ku.ac.th
Received 23 February 2024 / Accepted 17 June 2024

material (Kang *et al*., 2017). In the food industry, TCP is used in various applications such as anticaking and emulsifying. With rising demand, gastropod shell waste is becoming an attractive raw material for its synthesis (Seesanong *et al*., 2021).

TCP, consisting of a variable mixture of calcium phosphates with an approximate composition of $10CaO\text{-}3P_2O_5\text{-}H_2O$, is obtained from the neutralization of phosphoric acid (H_3PO_4) with calcium hydroxide ($Ca(OH)_2$) or $CaCO_3$ (European Union, 2020). The synthesis of TCP can be achieved through various methods, particularly thermal conversion and solid-state reaction methods (Bohner *et al*., 1997; Kang *et al*., 2017; Bohner *et al*., 2020). In this research, TCP was synthesized by the solid-state method through a chemical reaction between $CaCO_3$ or CaO and DCP at high temperature, as it is less intricate and consumes less energy. According to EU commission regulations regarding TCP specifications for food additives (E341 (iii)), neutralizing H_3PO_4 with $Ca(OH)_2$ or $CaCO_3$ produces DCP. $Ca(OH)_2$ is made from CaO and water, and CaO is derived from calcining $CaCO_3$. Direct use of $CaCO_3$ reduces production energy and the environmental impact of the production process, promoting a more sustainable approach (European Union, 2020).

This research aims to select and utilize $CaCO_3$ and CaO compounds derived from gastropod (*Murex* sp.) shell waste as starting materials for synthesizing TCP in a sustainable approach. However, there is no report comparing the product characteristics and environmental impacts of these starting materials, i.e. $CaCO_3$ and CaO, derived from gastropod shell waste and the relevant processes in the synthesis of TCP. In this study, life cycle assessment (LCA) is used as a comprehensive tool to estimate the total environmental impacts of TCP synthesis across all stages of its life cycle, from raw material extraction to waste management, aiding in the selection of eco-friendly materials and production methods (Hoffmann *et al*., 2012). The benefits of this research include reducing biowaste from gastropod and other seashell wastes, lowering energy consumption in production processes, and upcycling shell waste into valuable calcium compounds. This supports zero waste management and sustainable resource use in line with the Bio-Circular-Green Economy (BCG) model.

MATERIALS AND METHODS

Gastropod shell waste collection, preparation, and characterization

A gastropod (*Murex* sp.) shell sample was collected from a coastal area in Koh Chang, Trat Province, Thailand (Figure 1a). The shells were washed to remove silt and dirt from their surfaces and then naturally dried for 1–2 weeks (Figure 1b). After drying, the shells were crushed using a mortar and pestle and then sieved through a 0.045-mm mesh (Figure 1c). The composite was analyzed using the STA technique (449 F3 Jupiter, NETZSCH Group, Germany) to observe changes in structural and chemical compositions of the gastropod shell waste over a temperature range of 30–1,000 °C.

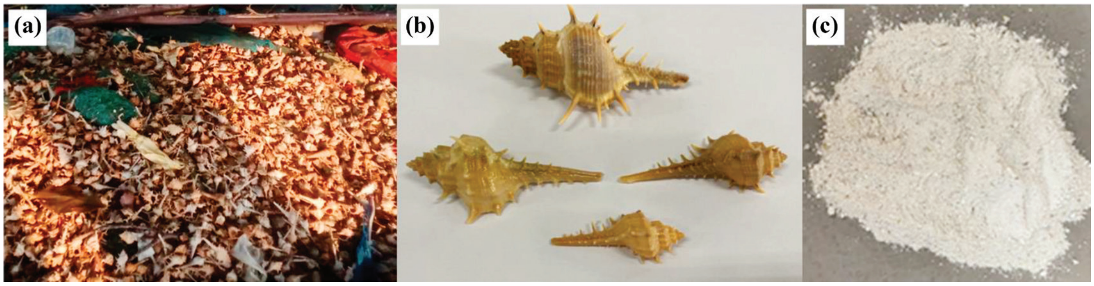

Figure 1. Gastropod shell waste used in the study (a) sample collection; (b) after cleaning; (c) after crushing.

Preparation of $CaCO_3$ and CaO from gastropod shell waste

To prepare $CaCO_3$, 25 g of dried shell was placed into a crucible and heated in an electric furnace at 300 °C for 1 h. to remove moisture, as the moisture is an important factor that allows organic matter to remain attached to the shell. The sample was then crushed using a mortar and pestle and sieved through a 0.045-mm mesh (Abanades *et al*., 2003; Carrier *et al*., 2016). The obtained $CaCO_3$ powder was stored in a desiccator until characterization using TOC (multi EA 4000, Analytik jena, Germany), XRF (S2 PUMA Series II, Bruker, USA), and XRD (D8 Advance, Bruker, Germany) with Profex 5.1.1 software for analysis of XRD patterns.

To prepare CaO, 10 g of dried shell was placed into a crucible and calcined in a furnace at 900 °C to convert the $CaCO_3$ in the shell to CaO (Galván-Ruiz *et al*., 2009). The sample was calcined for 30 min, then crushed using a mortar and pestle, and sieved through a 0.045-mm mesh. The obtained CaO powder, smaller than 45 µm was stored in a desiccator until characterization using XRD (Ramakrishna *et al*., 2018).

Synthesis of DCP

DCP was synthesized through a neutralization reaction involving $CaCO_3$ and H_3PO_4. Initially, 15 g of $CaCO_3$ powder derived from gastropod shell waste was dissolved with 600 mL distilled water. The slurry was stirred at a constant speed of 180 rpm, while the pH of the solution was adjusted to 5 by slowly adding 65% (v/v) H_3PO_4 (Nikolenko *et al*., 2020). The synthesized DCP was then separated from the mixture by vacuum filtration and stored in a desiccator to ensure dryness. Finally, the obtained DCP products underwent characterized using XRD and FT-IR (Frontier, Perkin Elmer, USA). Equation 1 illustrates the reaction of DCP synthesis from $CaCO_3$ (Kang *et al*., 2017):

$$CaCO_3+H_3PO_4 \rightarrow CaHPO_4+H_2O+CO_2 \quad (1)$$

Synthesis of TCP

The synthesis of TCP was carried out in two alternative ways, based on the starting materials derived from gastropod shell waste, namely $CaCO_3$ and CaO. $CaCO_3$/CaO and DCP powder were mixed at a ratio of 1:2. First, 5 g of DCP was completely dissolved in 200 mL of deionized water. Then, 2.5 g of $CaCO_3$ or CaO was added and stirred at 180 rpm at room temperature for 8 h. The precipitate was filtered using a vacuum filter and then incinerated at 900 °C for 30 min. The obtained TCP sample was stored in a desiccator prior to characterization using XRD and FT-IR. The reactions of TCP synthesis from different starting materials, i.e. $CaCO_3$ and CaO, are shown in Equations 2 and 3, respectively (Kang *et al*., 2017; Bohner *et al*., 2020).

$$CaCO_3+2CaHPO_4 \rightarrow Ca_3(PO_4)_2+CO_2+H_2O \quad (2)$$

$$CaO+2CaHPO_4 \rightarrow Ca_3(PO_4)_2+H_2O \quad (3)$$

Life cycle assessment (LCA)

LCA serves as a tool to examine the environmental impacts throughout the production processes. In this study, the analysis and comparison of the TCP production process using two alternative starting materials–$CaCO_3$ and CaO–were conducted following these steps:

Goal and scope and functional unit

The scope and units for the product analysis are established to assess the environmental impact of TCP production. By focusing solely on the production process, this study employed an LCA with a defined "gate-to-gate" system boundary and a functional unit of 1 g (Figure 2).

Life cycle inventory assessment (LCI)

LCI is a crucial procedure that assesses inputs and outputs of the TCP production process by quantifying raw materials and resource usage (including materials, energy, and chemicals) (Figure 3). The data from TCP synthesis were converted into inventory data and analyzed using Simapro software (version 9.2.0.2) to calculate the environmental impact of the production process. The analysis scope for this study is gate-to-gate, making it suitable for analysis using the IMPACT World+ midpoint V1.00/characterization method.

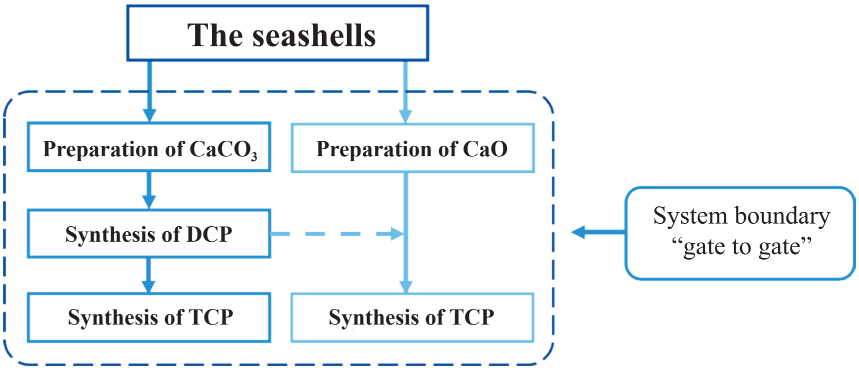

Figure 2. System boundary for LCA of 1 g TCP production.

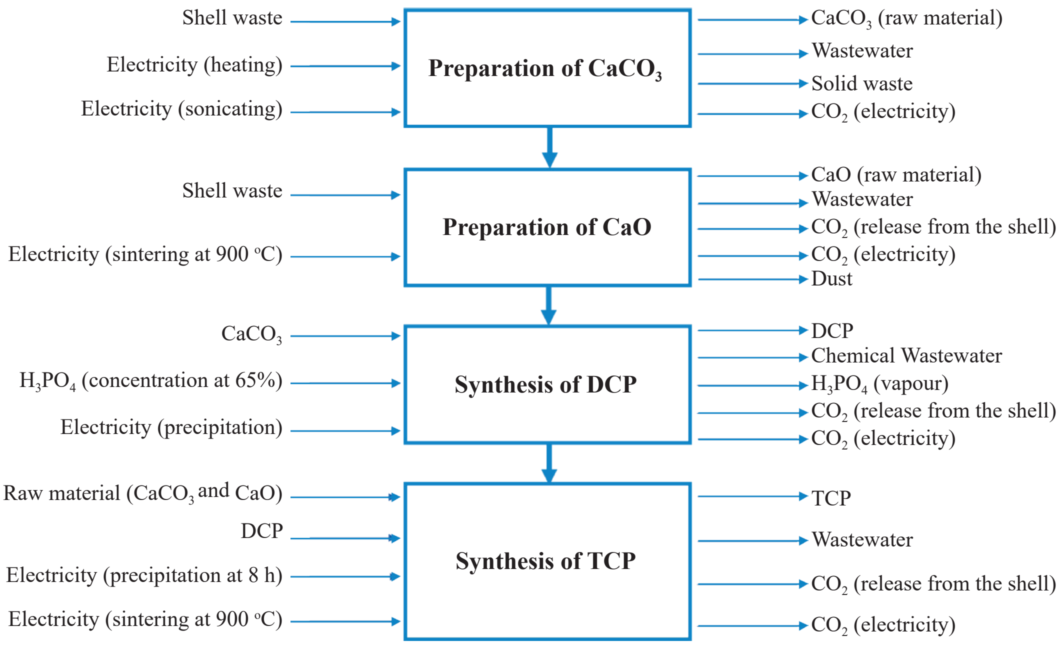

Figure 3. Inventory data for TCP synthesis.

RESULTS AND DISCUSSION

Characterization of composite from gastropod shell waste

The thermal behaviors of composites derived from gastropod shell were characterized using STA (Figure 4). The TG curve displayed a gradual decrease in gastropod shell mass from 75 °C, indicating moisture evaporation. A distinct transition occurred between 200 °C and 300 °C, signifying the complete removal of moisture and alteration of organic compounds within the shell. Subsequently, a significant change was observed at 560 °C, attributed to the organic substance decomposition. Mass loss continued until stability was reached at 830 °C, with a total loss of 55%, beyond which no further changes were observed. Both TG and DTG curves demonstrated the complete conversion of $CaCO_3$ to CaO above 830 °C, corroborating findings from Dampang *et al*. (2021).

Characterization of $CaCO_3$ prepared from gastropod shell waste

TOC analyzer was used to determine both inorganic and organic carbon present in the $CaCO_3$ sample extracted from gastropod shell waste. The average total carbon (TC) and inorganic carbon (IC) in the sample were 119.35 $g \cdot kg^{-1}$ and 118.65 $g \cdot kg^{-1}$, respectively, corresponding to the TOC content of 0.88 $g \cdot kg^{-1}$. Heating at 300 °C was found to remove some of the TOC from the gastropod shell waste, due to the partial decomposition of organic content. This result was consistent with Cho *et al*. (2021). As moisture is a key factor that facilitates the effective adherence of trace elements to the surface of the seashell, heating at 300 °C resulted in complete moisture loss, leading to the separation of trace elements from the seashell surface and facilitating the removal of organic contaminants from the composite (Mizuno *et al*., 2002; Wang *et al*., 2020).

XRF analysis of composites prepared from gastropod shell waste exhibited a substantial abundance of the Ca element, up to 99.08%, accompanied by the presence of other minor elements such as Na_2O, SiO_2, SO_3, K_2O, Sc_2O_3, Fe_2O_3, SrO, and TiO_2 (Table 1). This result indicated that the $CaCO_3$ in the composite prepared from gastropod shell waste met the criteria of $CaCO_3$ purity (>98%) regulated by general standard for food additives (GSFA) of Codex (170 i), as shown in Table 2. The result corresponded with Teawpanich (2021),

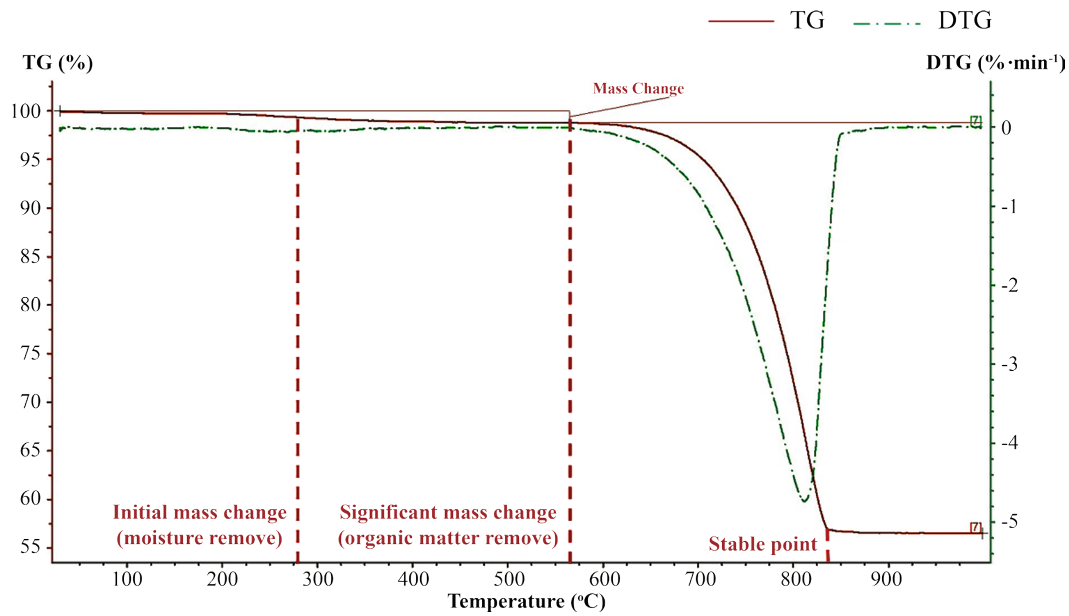

Figure 4. TG and DTG curves of the gastropod (*Murex* sp.) shell.

reporting that the purity of Ca in samples prepared through the heating method exceeded 98%. Additionally, the quality of the $CaCO_3$ composite was supported when comparing other parameters with commercial-grade $CaCO_3$ for the food industry, such as color (white powder) and Fe_2O_3 content (≤0.1%), as listed in Table 2. The findings confirmed that the $CaCO_3$ sample prepared from gastropod shell waste aligned with the specifications of international food standards and commercial products.

Figure 5a shows the image of the gastropod shell after cleaning and heating at 300°C, whereas the dried gastropod shell after crushing is illustrated in Figure 5b. The sieved $CaCO_3$ powder was subsequently analyzed by the XRD. Figure 5c depicts the XRD spectrum of the $CaCO_3$ composite prepared from gastropod shell waste. The result displayed high calcium content along with carbon and oxygen. The peaks at 2Θ of 23.10°, 29.45°, 31.40°, 36.01°, 39.47°, 43.21°, 47.52°, 48.55°, and 58.14° indicate the main crystalline phases of $CaCO_3$. This finding corresponds with the XRD pattern of calcite ($CaCO_3$) presented by Boudaira *et al.* (2015).

Characterization of CaO synthesized from gastropod shell waste

The gastropod shell was subjected to calcination at 900 °C, resulting in the production of CaO. Figure 6 shows the XRD pattern of CaO synthesized from gastropod shell waste after thermal treatment at a high temperature (900 °C). Based on the Profex 5.1.1 software, the diffraction peaks at 2Θ of 28.49°, 34.00°, 54.43°, and 71.89° are ascribed to CaO. These dominant peaks aligned with the XRD patterns reported by Lani *et al.* (2019). Additionally, the diffraction peaks at 2Θ of 18.59°, 47.04°, 50.79°, 59.51°, and 62.84° are indicative of $Ca(OH)_2$. As CaO is a highly hygroscopic material, it absorbs water from the atmosphere and converts to $Ca(OH)_2$ (Mohamed *et al.*, 2021). This result confirmed the conversion of $CaCO_3$ in the gastropod shell into CaO and $Ca(OH)_2$ phases due to the release of CO_2 from the shell. However, a trace amount of $CaCO_3$ was still observed with low-intensity peaks at 23.10°, 29.45°, 35.94°, 39.47°, 43.21°, and 48.55° as a result of incomplete conversion due to the limited time of calcination (30 min).

Table 1. XRF result of $CaCO_3$ composite prepared from gastropod shell waste.

Elements	**Percentage of oxide**
Na_2O	0.20%
SiO_2	0.34%
SO_3	0.06%
K_2O	0.02%
CaO	99.08%
Sc_2O_3	0.06%
Fe_2O_3	0.02%
SrO	0.22%
TiO_2	0.00%

Table 2. Comparison of obtained $CaCO_3$ with standard for food additives and commercial-grade food.

Properties	**This research**	**Codex (GSFA)[1]**	**Commercial-grade food[2]**
Color	white powder	white/colorless powder	white/colorless powder
$CaCO_3$	99.08%	>98%	>98%
Heavy metals	Fe: 0.02%	<0.03%	<0.03%
Particle Size	≤45 µm (0.045 mm)	≤65 µm	≤65 µm

Note: [1]GSFA = General standard for food additives (FAO, 2023); [2]Teawpanich (2021)

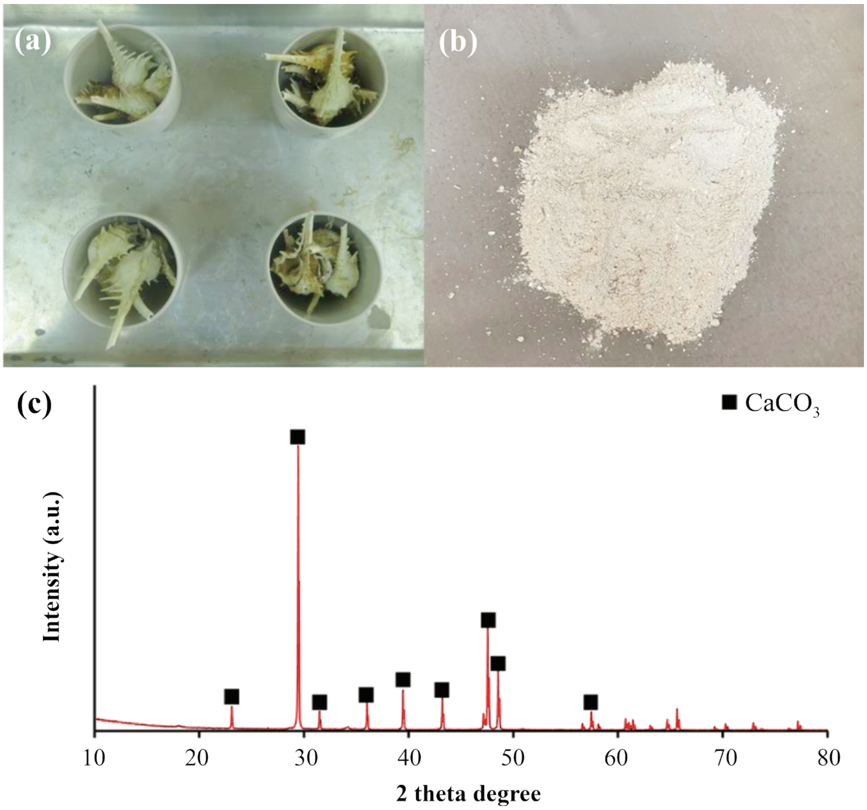

Figure 5. Appearance and physical characteristic of gastropod shell waste (a) dried specimen; (b) shell powder; (c) XRD spectrum of $CaCO_3$ composite prepared from gastropod shell waste.

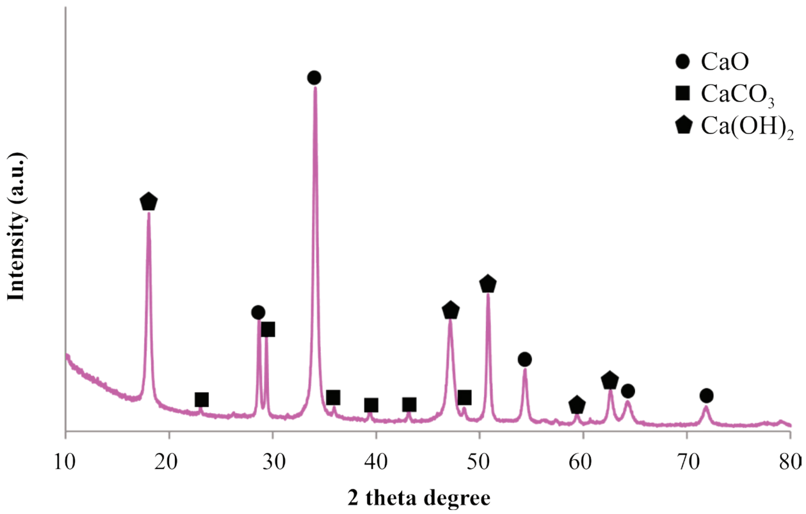

Figure 6. XRD pattern of CaO from gastropod shell waste after calcination at 900 °C.

Characterization of DCP derived from gastropod shell waste

DCP was synthesized through a neutralization reaction of H_3PO_4 and $CaCO_3$ from gastropod shell waste. Figure 7 shows the FT-IR spectrum in a wavenumber range of 4,000–600 cm^{-1} of the DCP products. The bands at 3,535 and 3,472 cm^{-1} were attributed to O–H stretching vibrations, originating from moisture in the sample. Additionally, H–O–H bending exhibited absorption at 1,645 cm^{-1}, while P-O stretching vibrations manifested at 1,198, 1,118 and 1,053 cm^{-1}, attributed to HPO_4^{2-} group of the DCP. Further characterization indicated P-O-P asymmetric stretching vibrations, observed at 982, 870, and 783 cm^{-1}, The FT-IR spectral data resembled the results reported by Yang *et al*. (2015). This finding confirmed the presence of functional groups in the DCP crystal structures.

Figure 8 depicts the XRD results of the DCP products derived from the gastropod shell waste. The prominent peaks at 2Θ of 11.85°, 20.86°, 23.33°, 29.60°, 30.49°, and 31.15° are indicative of DCP. These peaks mimic those observed by Lu *et al*. (2020) and Rafeek *et al*. (2021).

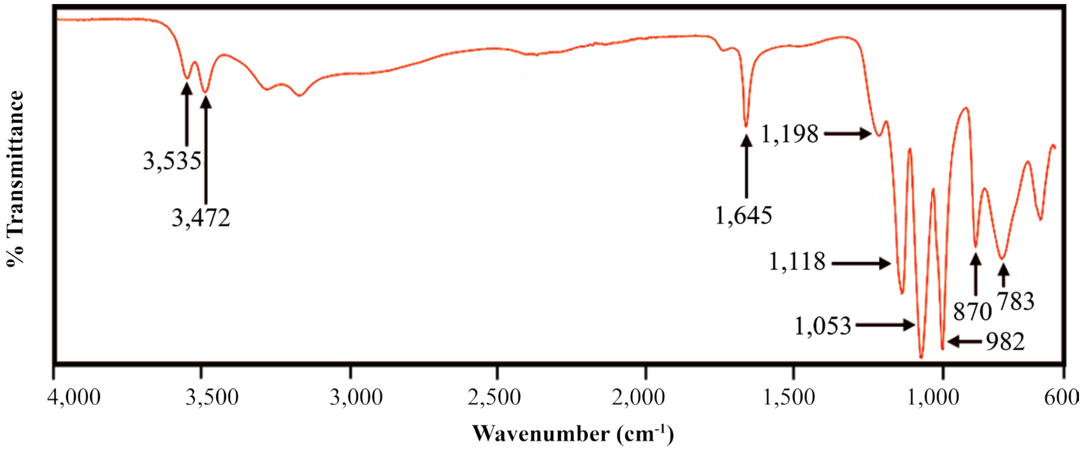

Figure 7. FT-IR spectra of DCP derived from gastropod shell waste.

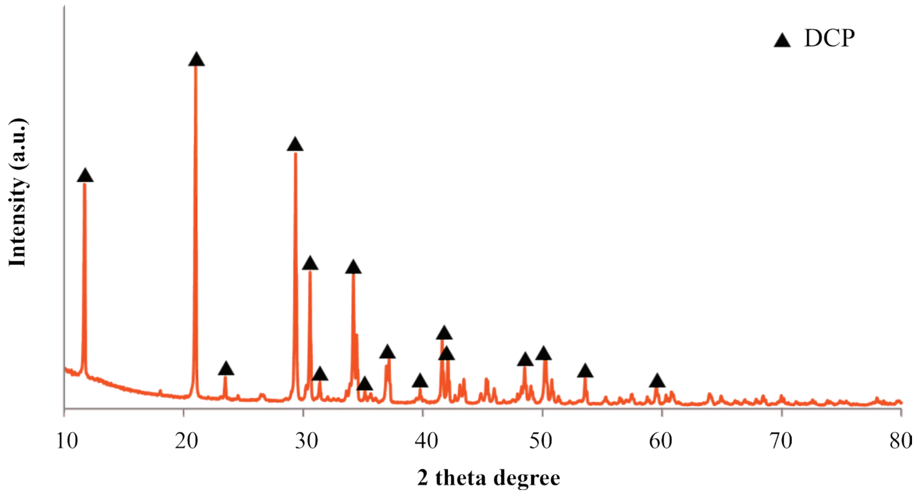

Figure 8. XRD pattern of DCP derived from gastropod shell waste.

Characterization of TCP derived from gastropod shell waste

TCP was produced through precipitation reaction of DCP with alternative materials derived from gastropod shell waste, namely $CaCO_3$ and CaO, over an 8 h period, followed by calcination at 900 °C for 30 min. Figure 8 shows the FT-IR results of the TCP products from both starting materials. The FT-IR spectra in the wavenumber range of 4,000–600 cm^{-1} exhibited subtle discrepancies. These variations in the spectra suggest the presence of O-H stretching vibrations and PO_4^{3-} ions. The distinctive bands at 3,643 and 3,572 cm^{-1} were attributed to O-H stretching, originating from moisture in the sample. The sharp peaks corresponding to the stretching modes of PO_4^{3-} ions were evident at 1,025 and 963 cm^{-1}, while those at 878, 875, and 630 cm^{-1} represented the vibration peaks of PO_4^{3-}. Furthermore, a minor peak at 1,457 cm^{-1} was detected during this phase, corresponding to a significant $CaCO_3$/CaO peak. This evidence suggested the presence of residual impurities from the raw materials (Kang *et al*., 2017; Dampang *et al*., 2021). The FT-IR spectra of TCP derived from $CaCO_3$ (Figure 9a) and CaO (Figure 9b) exhibited similarities and closely resembled those reported by Mehdikhani and Borhani (2014) and Zhang *et al*. (2005). These results confirmed the occurrence of the TCP derived from gastropod shell waste.

The XRD patterns of TCP derived from different starting materials from gastropod shell, i.e. $CaCO_3$/CaO, exhibited similar prominent peaks indicative of TCP at 2Θ of 25.73°/25.74°, 27.80°/27.79°, 30.97°/30.99°, 34.31°/34.37°, and 50.67°/49.44°, as shown in Figures 10a and 10b, respectively. Additionally, the diffraction peaks at 2Θ of 32.62°, 33.02°, and 39.31° were attributed to the presence of HA, while those at 2Θ of 18.50° and 34.00° were ascribed to CaO, as a raw material. HA was formed during heating in the range of 650–750 °C, whereas a small amount of CaO implied an incomplete reaction due to the short sintering time at 900 °C.

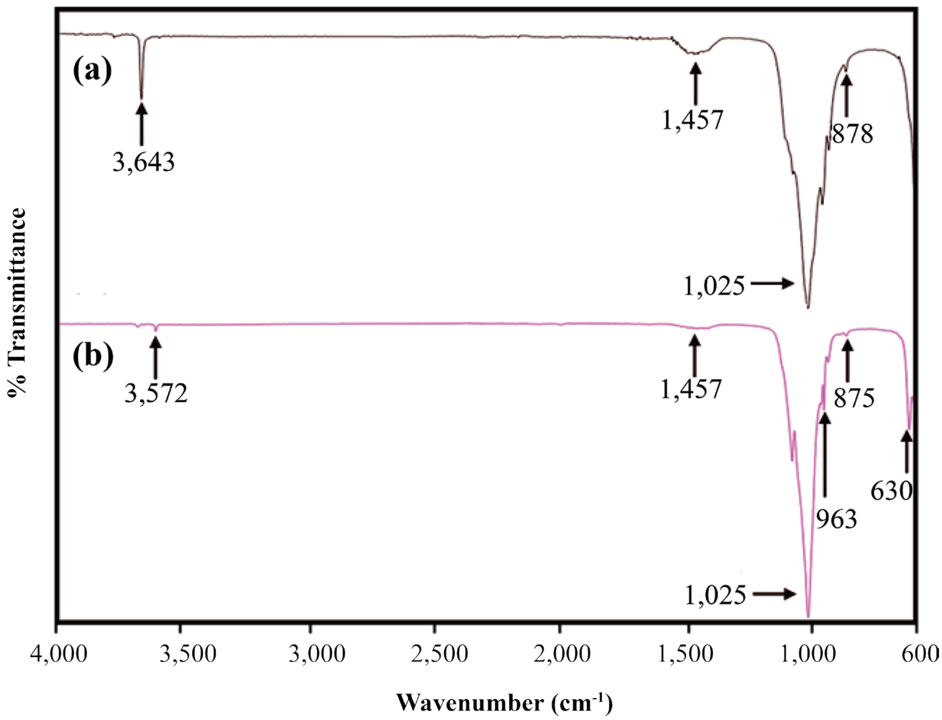

Figure 9. FT-IR spectra of TCP from: (a) $CaCO_3$; (b) CaO.

The XRD patterns corresponded with those presented by Tavares *et al*. (2013). A comparison of the XRD spectra between TCP produced from $CaCO_3$ and those from CaO revealed similar patterns of diffraction peaks, indicating that the TCP products synthesized using both raw materials did not exhibit any substantial difference in quality.

Life cycle assessment (LCA)

The inventory data, including input and output of materials and energy data, are listed in Table 3. After the output of inventory data was analyzed using Simapro software, it was categorized into possible midpoint effects on the environment and expressed in percentage terms as shown in Figure 11. The impact categories are identified as follows:

Dust generation

Dust is generated during the decomposition of shells at high temperatures in the preparation of raw materials, i.e. converting $CaCO_3$ to CaO. CaO being a fine particulate matter, can easily disperse in the air. It is categorized under a group with human toxicity effects (non-carcinogens) with % characterization of 100%, while dust from $CaCO_3$ is characterized as 81%.

Vapor or fumes

Vapor or fumes generated from the reaction between H_3PO_4 and $CaCO_3$ during DCP synthesis directly affect respiratory inorganics impact, where both raw materials exhibit the same impact ratio.

Chemical wastewater

Chemical wastewater containing H_3PO_4 generated during DCP synthesis directly influences both freshwater and terrestrial acidification. The results show that TCP production using CaO as a raw material causes a higher impact than that from $CaCO_3$.

Electricity utilization

Electricity used throughout the production processes originates from a diverse mix of sources (country mix), including natural gas and coal. It is categorized within the impact group of climate change (short-long term) (CaO = 100%, $CaCO_3$ = 81.9%) and fossil energy (CaO = 100%, $CaCO_3$ = 82.7%). The greater impact of CaO-synthesized TCP compared to $CaCO_3$-synthesized TCP is attributed to the production processes, which necessitates a higher usage of heat from electrical appliances.

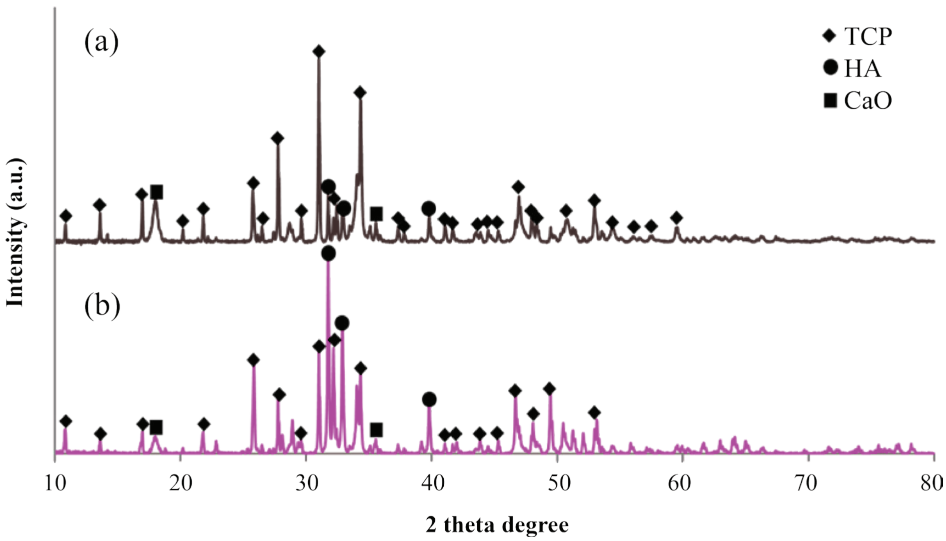

Figure 10. XRD patterns of TCP synthesized from different starting materials: (a) $CaCO_3$; (b) CaO.

Table 3. Inventory of material and energy data.

LCA stage	Input		Output	
Preparation of $CaCO_3$	Shell waste	25 g	$CaCO_3$ (raw material)	17.50 g (70% yield)
	Electricity (heating)	0.6 kWh	CO_2	0.2374 kg CO_2e
	Electricity (sonication)	0.04 kWh	Solid waste	(electricity)
			Wastewater	
Preparation of CaO	Shell waste	10 g	CaO (raw material)	5.90 g (59% yield)
	Electricity (calcination)	0.9 kWh	CO_2	0.0039 kg CO_2e (released from the shell)
			CO_2	0.3339 kg CO_2e (electricity)
			Wastewater	
			Dust	
Synthesis of DCP	$CaCO_3$	15 g	DCP	11.56 g (77.07% yield)
	65% (v/v) H_3PO_4	1.913 mL	CO_2	0.00345 kg CO_2e (release from the shell)
	Electricity (precipitation)	0.2 kWh	CO_2	0.0742 kg CO_2e (electricity)
			Chemical wastewater	600 mL
			H_3PO_4 (vapour)	
Synthesis of TCP	$CaCO_3$/CaO	2.5 g	TCP	4.60 g (61.33% yield)
	DCP	5 g	CO_2	0.00293 kg CO_2e (release from the shell)
	Electricity (precipitation)	1.6 kWh	CO_2	0.9275 kg CO_2e (electricity)
	Electricity (sintering)	0.9 kWh	Wastewater	

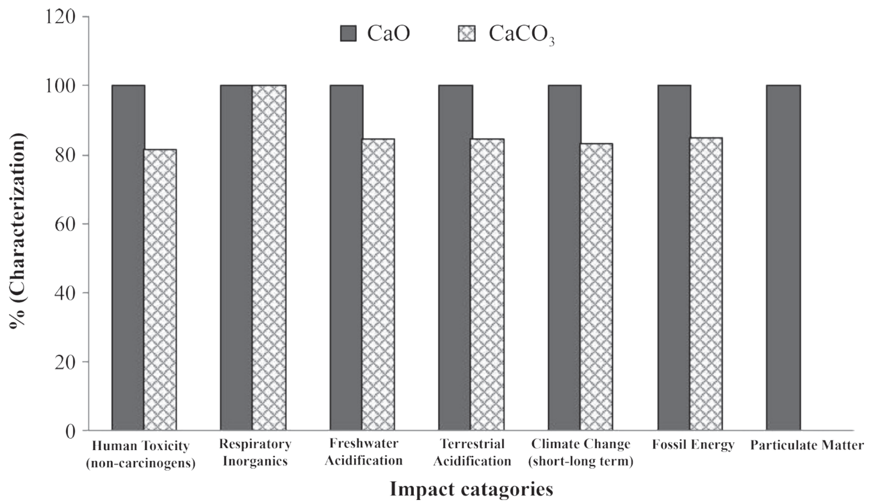

Figure 11. Comparison of life cycle impacts from TCP production processes using different starting materials derived from gastropod shell waste.

In this study, only the environmental aspect was taken into account. It is advisable to explore resource-efficient practices for mitigation of environmental impacts, such as using alternative materials and technologies in TCP manufacturing, which can reduce energy usage, emissions, and waste. Integrating life cycle analysis informs decisions by balancing sustainability and cost-effectiveness. Further study should include an economic analysis and social evaluation to achieve the sustainability of TCP manufacturing using gastropod shell waste as a raw material.

CONCLUSIONS

This research aimed to utilize $CaCO_3$ and CaO derived from gastropod (*Murex* sp.) shell waste as primary materials for synthesis of TCP as food additives. The results focused on selecting appropriate starting materials and sustainable production processes. The STA analysis of the gastropod shell waste indicated significant changes in the temperature range of 200–300 °C, primarily attributed to moisture removal. This corresponded with the TOC results, indicating that the shell underwent heat loss and partial decomposition of organic matter at 300 °C. Stabilization of mass loss occurred at 830 °C, indicating the complete transformation of $CaCO_3$ to CaO.

Characterization of the composite using TOC and XRF demonstrated that the physical characteristics of $CaCO_3$ met some criteria of the Codex general standard for food additives (GSFA), making it suitable for conversion into starting material for synthesizing TCP. Qualitative analysis with XRD and FT-IR confirmed that both $CaCO_3$ and CaO obtained were of the desired quality. The FT-IR and XRD data for DCP validated that the product resulting from the neutralization between $CaCO_3$ and H_3PO_4 was DCP. The TCP derived from precipitation and sintering between $CaCO_3$ or CaO with DCP was analyzed by FT-IR and XRD, revealing no noticeable difference in the quality and quantity of the synthesized yields.

The LCA demonstrated hotspots in TCP production associated with different raw materials. The choice of starting material in TCP production significantly influenced resource consumption, by-product generation, and overall environmental impact. The process employing CaO tended to consume more electrical energy, leading to increased CO_2 and dust emissions. Therefore the use of $CaCO_3$ derived from gastropod shell waste was proven to be a sustainable starting material for TCP production. However, in this study, only an environmental perspective was taken into account. Further study must include an economic analysis and social evaluation to achieve the sustainability of TCP production using gastropod shell waste as a raw material.

ACKNOWLEDGEMENT

This research was partially funded by the Department of Environmental Technology and Management, Faculty of Environment, Kasetsart University.

LITERATURE CITED

Abanades, J.C. and D. Alvarez. 2003. Conversion limits in the reaction of CO_2 with lime. **Energy and Fuels** 17(2): 308–315.

Azarian, M.H. and W. Sutapun. 2022. Biogenic calcium carbonate derived from waste shells for advanced material applications: A review. **Frontier in Materials** 9: 1024977. DOI: 10.3389/fmats.2022.1024977.

Bohner, M., J. Lemaıtre and T.A. Ring. 1997. Kinetics of dissolution of ß-tricalcium phosphate. **Journal of Colloid and Interface Science** 190(1): 37–48.

Bohner, M., B.L.G. Santoni and N. Döbelin. 2020. β-tricalcium phosphate for bone substitution: Synthesis and properties. **Acta Biomaterialia** 113: 23–41.

Boudaira, B., A. Harabi, F. Bouzerara, F. Zenikheri, L. Foughali and A. Guechi. 2015. Preparation and characterization of membrane supports for microfiltration and ultrafiltration using kaolin (DD2) and $CaCO_3$. **Desalination and Water Treatment** 57(12): 5258–5265.

Carrier, O., N. Shahidzadeh-Bonn, R. Zargar, M. Aytouna, M. Habibi, J. Eggers and D. Bonn. 2016. Evaporation of water: evaporation rate and collective effects. **Journal of Fluid Mechanics** 798: 774–786.

Cho, K., J. Kang, S. Kim, O. Purev, E. Myung, H. Kim and N. Choi. 2021. Effect of inorganic carbonate and organic matter in thermal treatment of mercury-contaminated soil. **Environmental Science and Pollution Research** 28(35): 48184–48193.

Dampang, S., E. Purwanti, F. Destyorini, S.B. Kurniawan, S.R.S. Abdullah and M.F. Imron. 2021. Analysis of optimum temperature and calcination time in the production of CaO using seashells waste as $CaCO_3$ source. **Journal of Ecological Engineering** 22(5): 221–228.

Department of Fisheries. 2022. **Marine capture production of commercial fisheries 2021.** https://www4.fisheries.go.th/local/file_document/20220526112717_1_file.pdf. Cited 24 Nov 2023.

el Biriane, M. and M. Barbachi. 2021. State-of-the-art review on recycled mussel shell waste in concrete and mortar. **Innovative Infrastructure Solutions** 6(1): 1–10.

European Union. 2020. **Commission regulation (EU) 2020/763.** https://eur-lex.europa.eu/legal-content/EN/TXT/PDF/?uri=CELEX:32020R0763. Cited 2 Jul 2022.

Food and Agriculture Organization of the United Nations (FAO). 2023. **Codex general standard for food additives (GSFA) online database.** https://www.fao.org/fao-who-codexalimentarius/codex-texts/dbs/gsfa/en/. Cited 20 Apr 2024.

Galván-Ruiz, M., J. Hernández, L. Baños, J. Noriega-Montes and M.E. Rodríguez-García. 2009. Characterization of calcium carbonate, calcium oxide, and calcium hydroxide as starting point to the improvement of lime for their use in construction. **Journal of Materials in Civil Engineering** 21(11): 694–698.

Hoffman, K., J. Skut, T. Skiba and J. Hoffmann. 2012. Life cycle assessment for industrial processes on the example of partially acidulated phosphate rocks. **Ecological Chemistry and Engineering A** 19(3): 301–309.

Iglikowska, A., J. Przytarska, E. Humphreys-Williams, J. Najorka, M. Chełchowski, A. Sowa, H. Hop, M. Włodarska-Kowalczuk and P. Kuklinski. 2023. Mineralogical and chemical composition of Arctic gastropods shells. **Progress in Oceanography** 218: 103134. DOI: 10.1016/j.pocean.2023.103134.

Kang, K.R., Z.G. Piao, J.S. Kim, I.A. Cho, M.J. Yim, B.H. Kim J.S. Oh, J.S. Son, C.S. Kim, D.K. Kim, S.Y. Lee and S.G. Kim. 2017. Synthesis and characterization of β-tricalcium phosphate derived from *Haliotis* sp. shells. **Implant Dentistry** 26(3): 378–387.

Lani, N.S., N. Ngadi, M. Jusoh, Z. Mohamad and Z.Y. Zakaria. 2019. Outstanding performance of waste chicken eggshell derived CaO as a green catalyst in biodiesel production: Optimization of calcination conditions. **Journal of Physics: Conference Series** 1349(1): 012051. DOI: 10.1088/1742-6596/1349/1/012051.

Lu, B.Q., T. Willhammar, B-B. Sun, N. Hedin, J.D. Gale and D. Gebauer. 2020. Introducing the crystalline phase of dicalcium phosphate monohydrate. **Nature Communications** 11(1): 1546. DOI: 10.1038/s41467-020-15333-6.

Mehdikhani, B. and G.H. Borhani. 2014. Densification and mechanical behavior of β-tricalcium phosphate bioceramics. **International Letters of Chemistry, Physics and Astronomy** 17(36): 37–49.

Mizuno, Y., F.K. King, Y. Yamauchi, T. Homma, A. Tanaka, Y. Takakuwa and T. Momose. 2002. Temperature dependence of oxide decomposition on titanium surfaces in ultrahigh vacuum. **Journal of Vacuum Science and Technology A: Vacuum, Surfaces, and Films** 20(5): 1716–1721.

Mohamed, F., M. Shaban, G. Aljohani and A.M. Ahmed. 2021. Synthesis of novel eco-friendly CaO/C photocatalyst from coffee and eggshell wastes for dye degradation. **Journal of Materials Research and Technology** 14: 3140–3149.

Nikolenko, M.V., K.V. Vasylenko, V.D. Myrhorodska, A. Kostyniuk and B. Likozar. 2020. Synthesis of calcium orthophosphates by chemical precipitation in aqueous solutions: The effect of the acidity, Ca/P molar ratio, and temperature on the phase composition and solubility of precipitates. **Processes** 8(9): 1009. DOI: 10.3390/pr8091009.

Rafeek, A.D., G. Choi and L.A. Evans. 2021. Controlled synthesis of dicalcium phosphate dihydrate (DCPD) from metastable solutions: Insights into pathogenic calcification. **Journal of Materials Science: Materials in Medicine** 32: 1–8.

Ramakrishna, C., T. Thenepalli, S.Y. Nam, C. Kim and J.W. Ahn. 2018. Extraction of precipitated calcium carbonate from oyster shell waste and its applications. **Journal of Energy Engineering** 27(1): 51–58.

Seesanong, S., B. Boonchom, K. Chaiseeda, W. Boonmee and N. Laohavisuti. 2021. Conversion of bivalve shells to monocalcium and tricalcium phosphates: an approach to recycle seafood wastes. **Materials** 14(16): 4395. DOI: 10.3390/ma14164395.

Tavares, D.D.S., L.D.O. Castro, G.D.D.A. Soares, G.G. Alves and J.M. Granjeiro. 2013. Synthesis and cytotoxicity evaluation of granular magnesium substituted β-tricalcium phosphate. **Journal of Applied Oral Science** 21: 37–42.

Teawpanich, P. 2021. **Quality control of chemical grade calcium carbonate from Lopburi limestone deposit in Thailand.** Master Thesis, Chulalongkorn University, Bangkok, Thailand. 56 pp.

Wang, Z., L. Xia, J. Chen, L. Ji, Y. Zhou, Y. Wang, L. Cai, J. Guo and W. Song. 2020. Fine characterization of natural SiO_2-doped catalyst derived from mussel shell with potential photocatalytic performance for organic dyes. **Catalysts** 10(10): 1130. DOI: 10.3390/catal10101130.

Yang, C., K. Lin and J. Chang. 2015. A simple way to synthesize 3D hierarchical HAp porous microspheres with sustained drug release. **Ceramics International** 41(9): 11153–11160.

Yinka, K.M., A.J. Olayiwola, A. Sulaiman, A. Ali and F. Iqbal. 2020. Preparation and characterization of hydroxyapatite powder for biomedical applications from giant African land snail shell using a hydrothermal technique. **Engineering and Applied Science Research** 47(3): 275–286.

Zhang, Y., G. Yin, S. Zhu, D. Zhou, Y. Wang, Y. Li and L. Luo. 2005. Preparation of β–$Ca_3(PO_4)_2$ bioceramic powder from calcium carbonate and phosphoric acid. **Current Applied Physics** 5(5): 531–534.